JOURNAL OF MATERIALS SCIENCE 31 (1996) 6555–6563

Synthesis of a nanophase, whisker-reinforced, ceramic/metal composite by electrochemical infiltration

T. J. LEE, K. G. SHEPPARD, Y. Q. LI*, B. GALLOIS
Department of Materials Science and Engineering, Stevens Institute of Technology, Hoboken, NJ 07030 USA

A novel, nanophase metal-matrix composite sheet material has been synthesized. Nickel was infiltrated by electrodeposition into a "wool-like" mat of SiC whiskers that had been grown by chemical vapour deposition. Infiltration of nickel by d.c. plating, pulse plating, and the effects of a tin–palladium surface treatment of the SiC whiskers were evaluated. Pulse plating combined with the Sn–Pd treatment were effective in minimizing porosity. Compared to values for the unreinforced electrodeposited nickel, the hardness could be almost quadrupled and the wear rate decreased to approximately one sixth in a composite with $\approx$30 vol % whiskers.

1. Introduction

Metal matrix composites (MMCs) have attracted considerable interest because of their superior mechanical [1] and tribological [2] properties. Such composite materials can be fabricated by various means such as by melt infiltration, powder metallurgy [3, 4] or electrodeposition [5–11]. Compared to the unreinforced metals, MMCs generally exhibit greater wear resistance, hardness, stiffness (Young's modulus), strength, good impact resistance, lower density and good dimensional stability.

There are a number of advantages to using electrodeposition to synthesize MMCs. Electrocomposites do not require high temperatures or pressures during processing. A variety of shapes and thicknesses can be produced with little or no post-machining [12]. The composite can be in the form of a coating or a removable mandrel is used to prepare electroforms [13].

Typically, the composite is produced by the co-deposition of fibres or particles that have been suspended in the electrolyte used to plate the matrix. Another approach involves winding a continuous filament onto a rotating cathode during electrodeposition of the matrix. For example, Withers and Abrams [8] describe electroformed nickel-matrix composites containing up to 50 vol % tungsten, boron or SiC fibres. They also were able to electroform composites with 10 vol % SiC whisker rovings. Additionally, copper and aluminium matrix composites were produced. Ahmad *et al.* [9] have electroformed a variety of nickel-matrix composites, including ones containing up to 6% SiC whiskers that had been suspended in the plating bath. They experienced difficulty with void formation and its detrimental influence on mechanical properties. A general characteristic found with co-deposition of freely suspended whiskers, is their tendency to incorporate in the deposit with the whisker axis parallel to the surface. Reinforcement is thus only two dimensional.

Electrodeposition has also been used to coat metal onto fibres prior to consolidation into bulk composites [14]. While the material produced by this approach has exposure to heat and pressure, electrodeposition still offers advantages over other processing routes in that it allows for uniform separation of the fibres. It also allows pre-coating of the fibre with a diffusion barrier or a graded coating to better match thermal expansion coefficients and tailor the mechanical properties for optimal reinforcement.

In this paper we report on a different approach to electroforming SiC whisker-reinforced, metal-matrix composites. The whiskers are grown in the form of a "wool-like" mat by chemical vapour deposition (CVD) onto a graphite substrate. The whiskers have diameters that can be controlled in the approximate range 30–400 nm. We have employed electrodeposition to infiltrate the mat to form a nickel-matrix composite. This is possible because the graphite substrate used to grow the whiskers can form the cathode in an electrodeposition cell. The aim was to grow the nickel from the substrate outwards to the mat surface. The advantage of using the whisker mat is that the three-dimensional orientation of the whiskers produces a composite with more isotropic reinforcement than obtained from whiskers suspended in the electrolyte. This approach is also capable of producing greater ceramic loading than obtainable by co-deposition of ceramic particles that are suspended in the electrolyte, the typical route to electroformed, metal matrix composites. Infiltration by both direct current and pulse

* Presently with NZ Applied Technologies Inc., Woburn, MA

0022–2461

plating have been studied as well as pretreatment of the whiskers with a tin–palladium seed layer.

SiC whiskers can be prepared by CVD, utilizing either vapour–solid (VS) [15, 16] or vapour–liquid–solid (VLS) [17] mechanisms. The latter involves whisker growth that is catalysed by a molten metallic droplet that resides at the tip of the whisker throughout its evolution. The SiC whisker mat that we have infiltrated was prepared using a new variation on the VLS approach. As the present paper focusses on the infiltration aspects, we provide only an overview of the whisker growth here, the process is described in detail elsewhere [18].

2. Experimental procedure

2.1. SiC whisker preparation

The SiC whiskers were deposited in a hot-wall CVD reactor shown schematically in Fig. 1. A horizontal quartz tube was heated to 1425 °K by a resistive furnace and the pressure controlled by a mechanical pump and needle valve connected to a pressure controller. Mass flow controllers were used to control the reactant gases in the system. The precursor methyltrichlorosilane (MTS = CH_3SiCl_3) was used as the source of both silicon and carbon. The MTS was held at a temperature of 273 °K in an ice bath. Hydrogen was used as both the carrier gas and as the reducing agent for the MTS.

A new approach used in the present work was to supply the nickel catalyst, needed to facilitate VLS growth of SiC whiskers, via the gas phase. VLS growth reported by others employed metallic catalysts that had been directly deposited onto the substrate prior to whisker growth. Our approach using the gas phase to supply the catalyst has the potential advantage of scalability. In the present work, nickel was introduced into the gas stream by positioning a nickel sheet upstream from the graphite substrate. The nickel reacts with the products of decomposition of MTS to form nickel chloride which is volatile at the deposition temperature. A liquid alloy droplet of Ni–Si–C is subsequently formed at the substrate surface and the SiC whiskers grow from these droplets by means of the VLS mechanism. The conclusion that this mechanism is operating is supported by energy dispersive X-ray analysis performed in the scanning transmission electron microscope on droplets at the tips of whiskers. This showed that the droplets contained nickel, silicon and carbon.

It is found that the density of SiC whiskers decreased with increasing thickness of the mat, as seen in Fig. 2. The diameters of SiC whiskers and the mat thickness were a function of processing conditions (Fig. 3). Diameters from 30–400 nm could be obtained and the mat thickness obtained in one hour ranged from 0.15 to almost 1 mm.

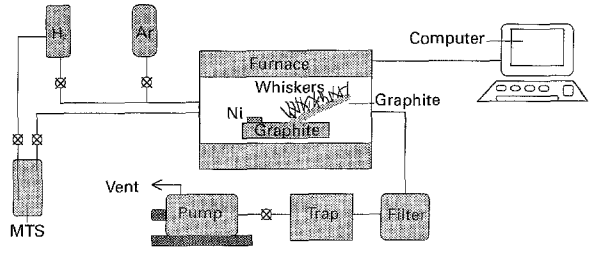

Figure 1 Schematic illustration of the hot-wall CVD system.

2.2. Electrochemical infiltration of whiskers

The SiC wool on graphite can be considered to be a porous, reticulate electrode. In such electrodes the mass transfer rate and current distribution for electrochemical processes are influenced by the electrolyte

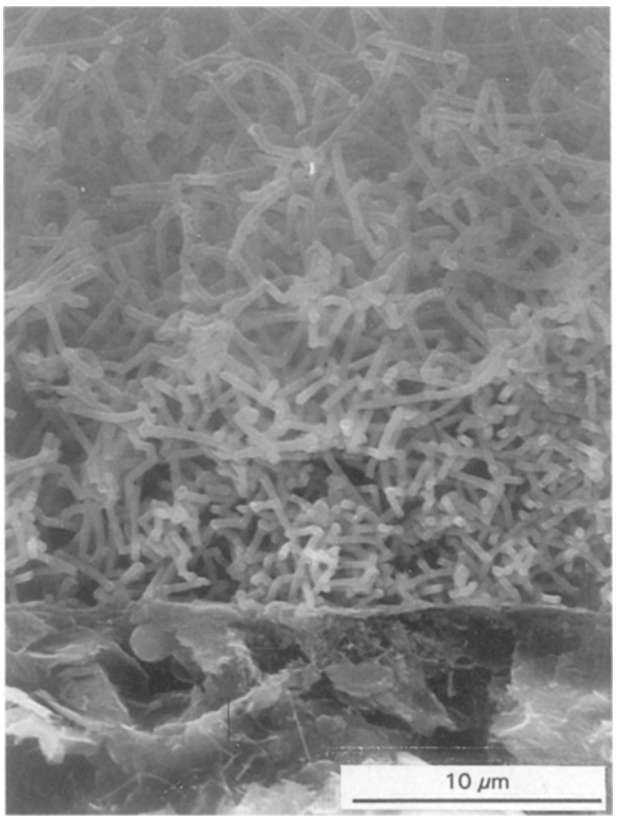

Figure 2 Cross-sectional view of SiC whisker mat on graphite substrate.

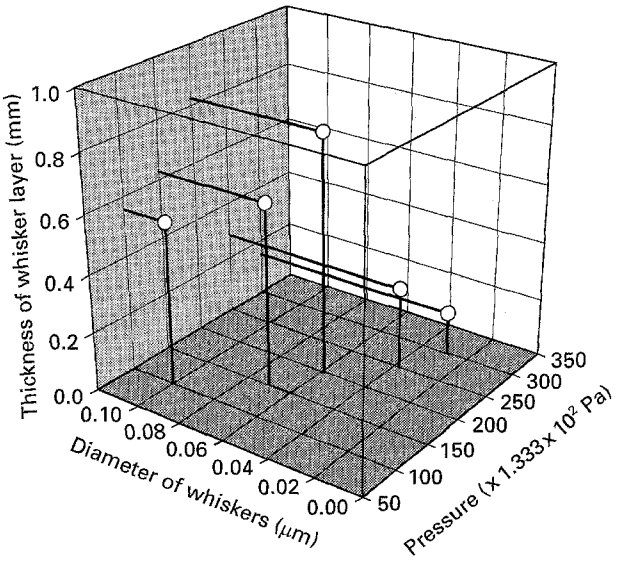

Figure 3 Whisker growth dependence on processing conditions.

flow and the relative directions of electrolyte flow and current [19, 20]. We have experimented with several modes of agitation and found that bubbling air was the most effective. The sample size was 1.1 cm × 1.1 cm.

The electrodeposition current was controlled using a potentiostat/galvanostat (Princeton Applied Research Model 173). Both d.c. and pulsed current plating were investigated. The pulse parameters were controlled by a waveform generator (Princeton Applied Research Model 175) coupled to the potentiostat.

Plating was performed in a standard Watts nickel plating bath containing nickel sulphate (225 g per l), nickel chloride (37.5 g per l) and boric acid (30 g per l). The bath was operated at a temperature of 48 °C and a pH 3.5. The d.c. plated specimens were plated at a current density of 5 mA cm^{-2}. Pulse plating was at 5 mA cm^{-2} average current density, with a 10% duty cycle at 100 Hz. Triton X-100 (0.9 ml per l) was used in some experiments. This is a proprietary (Rohm and Haas) polymeric non-ionic surfactant that is commonly used in plating electrolytes to reduce gas porosity and inhibit dendritic growth. It has the formula $C_8H_{17}(C_6H_4)(OCH_2CH_2)_xOH$(x = 9–10) and molecular weight of 628.

2.3. Surface modification of SiC whiskers

As a strategy to reduce porosity following infiltration with nickel, some of the SiC samples were treated to change the surface condition of the whiskers. The samples were immersed at room temperature for three minutes in a solution of tin chloride (10 g per l $SnCl_2$, 40 ml per l conc. HCl), rinsed in distilled water, immersed in palladium chloride solution (450 mg per l $PdCl_2$, 30 ml per l conc. HCl) for three minutes and then rinsed again. This is a treatment used in electroless plating of non-conducting surfaces to produce catalytic Sn–Pd clusters on which autocatalytic deposition can initiate. While in the present work autocatalytic deposition was not employed, as we will show, the surface treatment had a beneficial effect on the infiltration process.

2.4. Characterization of the composites

Samples before and after infiltration were examined in cross-section by scanning electron microscopy (SEM). Composite samples were also mechanically polished to a 0.05 μm alumina finish, both in cross-section and parallel to the surface, to reveal the extent of porosity. The average crystallite size of the nickel matrix was estimated from Warren–Averbach line broadening analysis applied to X-ray diffraction measurements (Siemens Model D-5000). Transmission electron microscopy (TEM) (Philips EM400) was also used to observe the matrix grain size.

Some initial evaluation has been performed on the property enhancement achieved by incorporating the SiC whiskers into nickel. We have measured hardness and wear behaviour as a function of the volume fraction of whisker reinforcement. In these measurements we have taken advantage of the fact that with the present stage of our technology, the density of whiskers decreases as the distance from the substrate increases. By polishing the composite samples at a shallow angle to form a wedge extending from the substrate to the surface, different depths through the composite were exposed and hence regions of differing whisker volume fraction were obtained with a single sample.

The Knoop microhardness (200 g load) was measured at different locations with varying whisker fraction (Leco Microhardness Tester Model M400-G2). The wear measurements were performed using a pin-on-disc machine. A 52100 steel ball was rubbed against a rotating disk of the taper-polished composite specimens. All specimens were tested under the same conditions: sliding speed = 1 cm per s; load = 500 g; sliding distance = 110 m. The amount of material removed by wear at different points on the circular wear track was measured as a volume loss, using a profilometer to measure the track wear profile.

An image analysis technique was employed to determine the whisker volume fraction at each location where a hardness or wear track profile measurement had been performed. SEM was used to obtain a digitized image of each location. Image analysis software routines (NIH-Image 1.45 by Wayne Rasban, National Institutes of Health) then allowed grey scale adjustment followed by conversion to a black and white (binary) image that discriminated the whiskers from the matrix. From this image the volume fraction of whiskers could be obtained.

3. Results and discussion

3.1. D.c. plating

It was observed that initially the nickel grew from the substrate in a uniform manner towards the surface of the mat. However, as deposition progressed, isolated balls of nickel formed on some whiskers away from the substrate as is shown in Fig. 4. It is possible that a small leakage current through the whiskers initiated local deposition. This was likely followed by rapid hemispherical diffusion that promoted growth of the balls. While pure single crystal SiC is a wide band-gap semiconductor (2.8 eV for α-SiC, 2.2 eV for β-SiC), because of crystal defects and impurities it has been found that electrical resistivities as low as 10^{-3} Ω cm can be obtained in SiC whiskers [21]. This is the same order of magnitude as the resistivity of graphite. Hence, leakage current through the whiskers is a possibility.

At longer infiltration times, impingement of the balls growing on the sides of whiskers led to occlusion of uninfiltrated regions in the whisker mat. Thus, ionic transport of metal to these regions was cut off leading ultimately to porosity. Fig. 5 shows an SEM micrograph of a polished section parallel to the surface from a d.c. infiltrated composite. One can observe large and small pores in addition to features that look like cracks in the nickel matrix. The pores are due to the occlusion from the impinging growths on the whiskers and also possibly due to trapped hydrogen bubbles (there is hydrogen evolution as part of the nickel electrodeposition process). The crack-like defects are

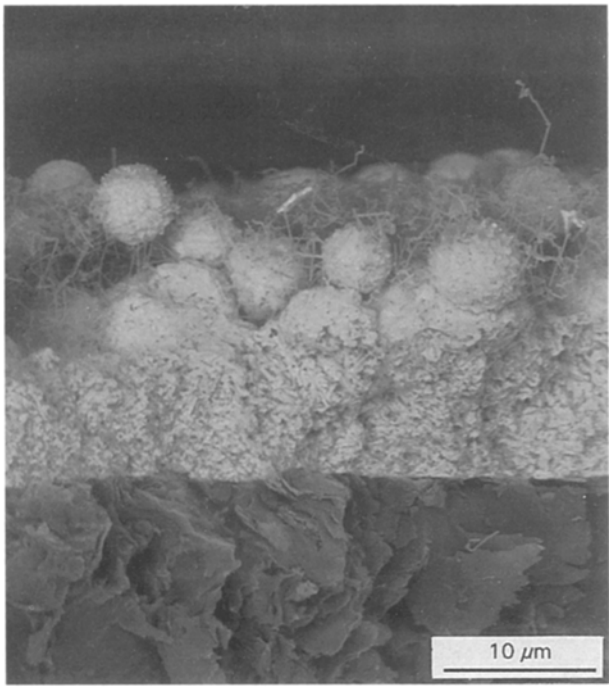

Figure 4 Cross-sectional view of partially infiltrated mat using d.c. plating.

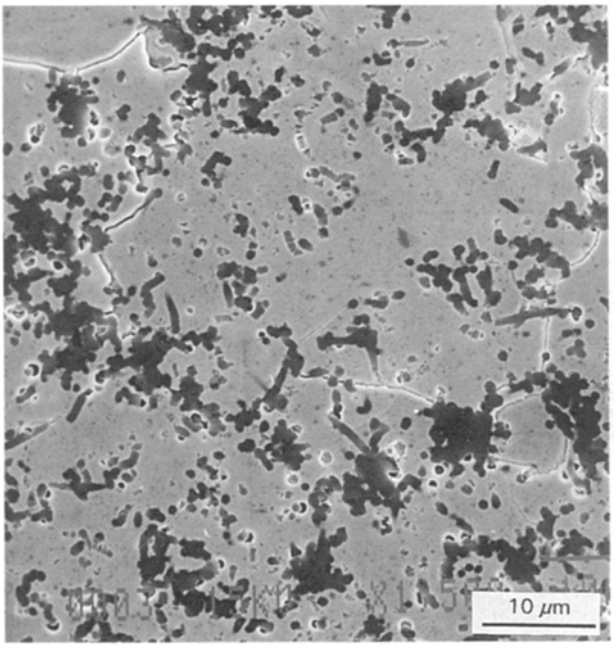

Figure 5 Polished section parallel to surface of a d.c. infiltrated sample.

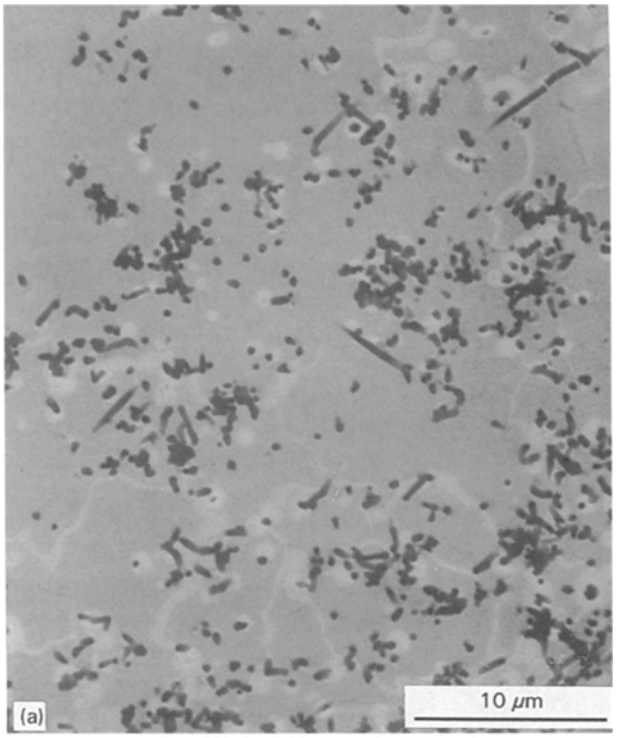

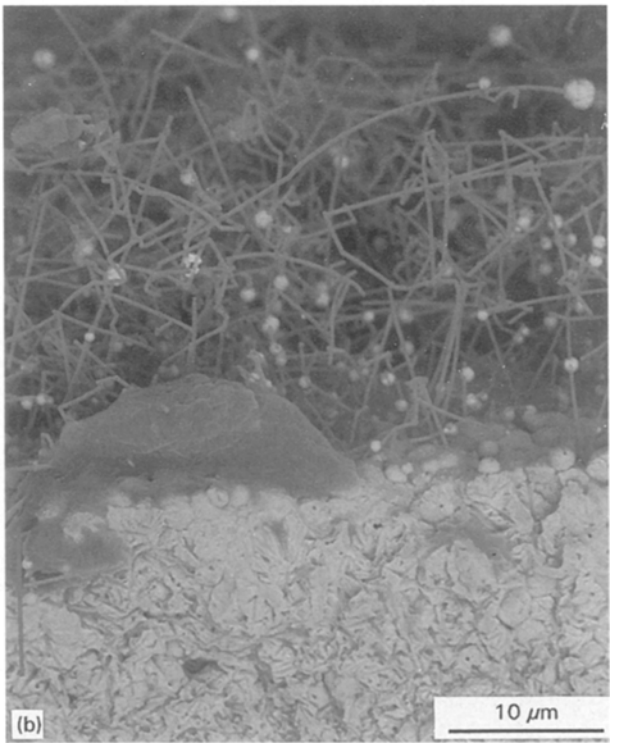

Figure 6 (a) polished section of fully infiltrated sample by pulse plating (b) cross-section of partially infiltrated sample.

likely due to incomplete joining where impinging nickel outgrowths from the whiskers met.

3.2. Pulse plating

Fig. 6a is a polished section parallel to the surface showing that a significant reduction in porosity was achieved by the use of pulse plating. A few small pores remain that are located at the whisker/matrix interface. Fig. 6b is a cross-sectional view of a sample after partial infiltration by pulse plating. It is seen that the nickel balls are significantly smaller than those produced by d.c. plating, however, their number increased. The smaller outgrowths on the whiskers did not cause an impediment to the infiltration process and therefore did not induce porosity.

Employing pulse plating in order to reduce porosity due to ball formation has a potential secondary benefit. It has been found by others that pulse plating conditions that favour grain refinement also lead to a reduction in electrodeposit porosity compared to direct current plating [22]. The porosity that is reduced is typically due to hydrogen gas bubbles.

The improvements obtained by pulse plating can be explained when one considers its effects on the interplay between nucleation and growth in the deposit. Overpotential, i.e., the deviation of the electrode potential from its equilibrium value, can be considered a measure of the supersaturation when a deposition process is driven at an electrode surface by passage of a cathodic current. High values of overpotential are associated with a high population of adions at the surface, i.e., ions that reside on the surface but are not yet fully discharged and incorporated in the metal. Limited surface diffusion is also characteristic. These conditions typically arise due to the combination of a high flux of discharging ions, combined with the presence of adsorbed species that may block the favoured growth sites such as ledges and kinks, and/or absorb uniformly and impede surface diffusion. High overpotential conditions therefore favour three-dimensional nuclei formation rather than the continued growth of existing layers [23].

In pulse plating the peak current density and hence the overpotential is considerably larger than for d.c. plating at the same average current density. The large overpotential during the on-time, together with an off period prior to the next deposition pulse, combine to produce repeated nucleation rather than growth of existing nuclei [23]. For this reason, the growth of nickel on the whiskers under pulse conditions promotes more numerous nuclei rather than the large scale growth of the few initial nuclei seen with d.c. plating. An additional mechanism by which porosity may be reduced by pulse plating is repeated nucleation that allows voids between crystallites to be filled [24]. In d.c. plating the continued growth of existing nuclei can lead to bridging over of voids leading to microporosity.

The repeated nucleation of pulse plating also leads to a finer grain structure in the nickel matrix. Fig. 7 contains TEM micrographs that reveal the nickel matrix grain structure obtained by both pulse and d.c. plating. The dark-field images show the pulse-plated material has a significantly smaller grain size. TEM only examines a limited area. The X-ray line broadening analysis (Warren–Averbach method [25]) provides an assessment of the coherently diffracting domain size averaged over a large area. This is shown in

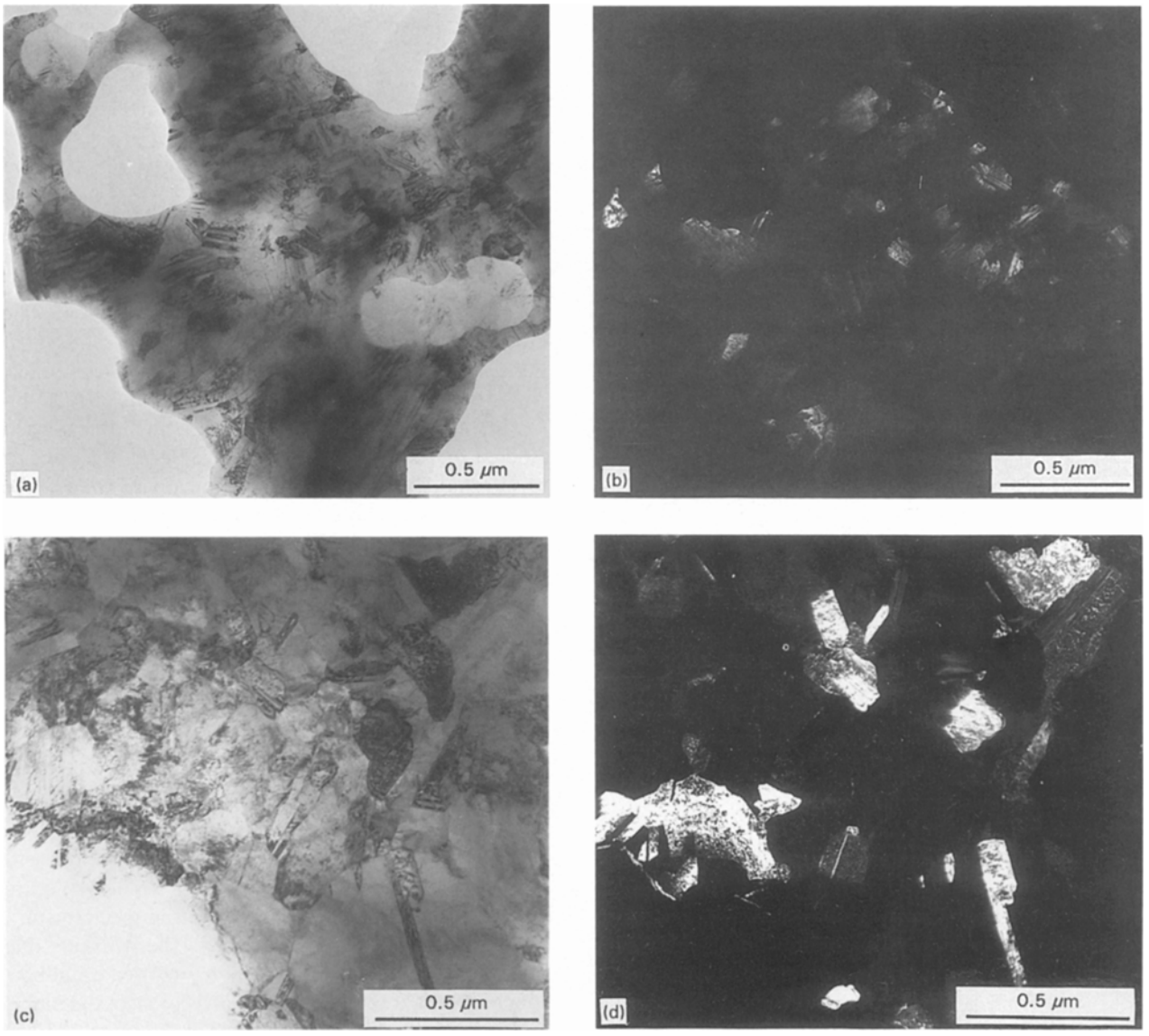

Figure 7 TEM of nickel matrix (a) bright field, pulse plated (b) dark field (111), pulse plated (c) bright field, d.c. plated (d) dark field (111), d.c. plated.

Fig. 8(a and b). Particle size broadening of the {111} and {222} diffraction peaks of nickel was deconvoluted from microstrain effects [25] to reveal the average crystallite size in the direction normal to the surface (cf. TEM gives the grain size in the plane of the surface). Fig. 8a shows the average coherent crystallite size from a pulse-plated sample to be 53 nm. The plot is of the size broadening contribution to the Fourier cosine coefficients (A_n) of broadened peaks against averaging length L normal to the diffracting planes. Extrapolation of the initial slope to the length axis gives the crystallite size. Several such measurements gave 50 ± 10 nm. D.c. plated samples (e.g. Fig. 8b) gave 460 ± 40 nm, i.e., an order of magnitude larger. These numbers are consistent with the dark field TEM results.

We do not know to what extent the porosity seen from d.c. plating was due to hydrogen gas. Atomic hydrogen is discharged during nickel plating and can then combine to form gas bubbles. These bubbles can be trapped at the advancing matrix surface or by the whisker network and subsequently occluded, leading to pore formation. Pulse plating can reduce this source of porosity by allowing desorption during the off-time after each pulse, thus limiting bubble formation [26].

3.3. Effect of surfactant

The addition of the surfactant, Triton X-100, had some beneficial influence with d.c. plating. There was a substantial increase in the number of balls that nucleated on the whiskers and they were significantly reduced in size compared to plating without the additive. This is likely a result of the increased deposition overpotential that results from adsorption of the surfactant and the consequent hindrance of continued growth of existing nuclei. The overpotential is raised sufficiently to initiate more widespread nucleation. However, the additive effect was not as favourable as that of pulse plating. The change in throwing power by the surfactant adsorption was not sufficient to allow the deposit to grow out through the whisker network without closure from the growing balls. Thus the final composite had porosity, although reduced from that of d.c. plating without the additive.

Combining current pulsing with the presence of a surfactant in the electrolyte improved the deposit compared to d.c. plating, however it retained more porosity than pulsing in the absence of the additive. The reason why the additive made pulsing less effective is not clear. The interplay of the large transient deposition flux during the on-pulse followed by relaxation by diffusion in the off-pulse could influence additive transport, adsorption and incorporation into the deposit in a manner that produced poorer throwing power than if the additive had not been present.

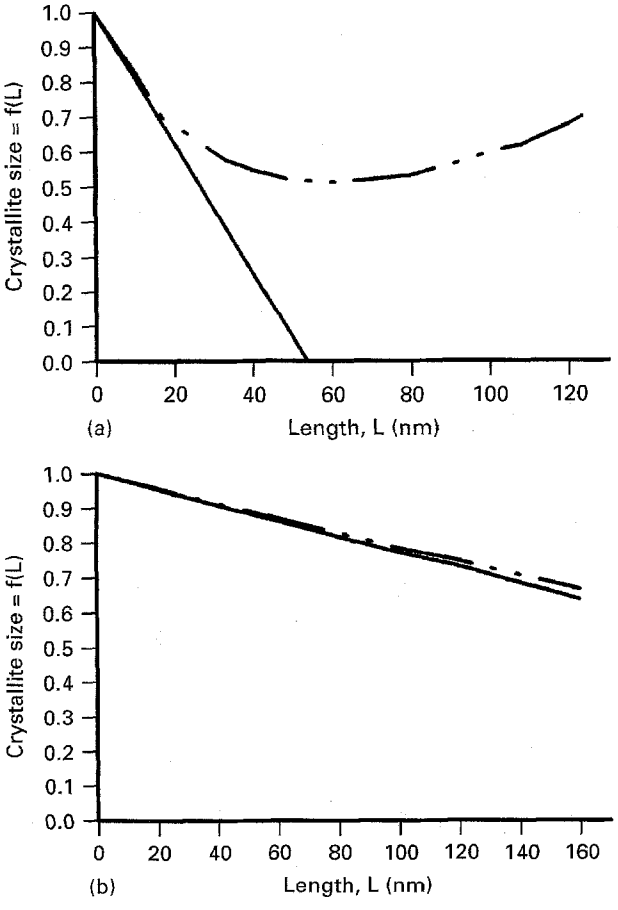

Figure 8 Crystallite size of nickel matrix measured by X-ray techniques (a) pulse plated, (b) d.c. plated.

3.4. Whisker surface modification

Even with pulse plating some residual porosity remained, mostly at the whisker/matrix interface. This prompted us to try whisker surface modification with a Sn/Pd treatment. The result is shown in Fig. 9a. It is seen that the whiskers are uniformly coated with nickel, rather than with localized balls of metal. The uniform whisker coating appears to have eliminated the residual porosity at the whisker/matrix interface. A section parallel to the surface is shown in Fig. 9b.

The seeding of silica glass with Sn/Pd has been studied by de Minjer and van den Boom [27]. Their results indicated that tin was chemically bonded to the Si–O groups of the glass surface, with the palladium present as a tin–palladium complex having excess tin, rather than as metallic palladium. It is not clear in our work if the Sn/Pd changed the surface contact characteristics, inducing more uniform charge transfer at the whisker/electrolyte interface, i.e., deposition current flowing through the whiskers. Alternatively, the tin–palladium clusters, typically produced by the Sn/Pd treatment, may have facilitated enhanced growth of nickel along the whiskers starting from the substrate. This could have occurred by a "hopping mechanism" in which bridging occurred between Sn/Pd clusters, with growth along the whiskers occurring preferentially to that normal to the whisker surface. We are studying this further to understand the mechanism.

The uniform growth initiated on the whiskers due to Sn/Pd seeding appears to have provided an adherent coating that then grew outwards to meet the nickel infiltrating from the substrate to fill the inter-whisker space. Without the coating, nickel impinging on the bare whisker surface may have not adhered well due

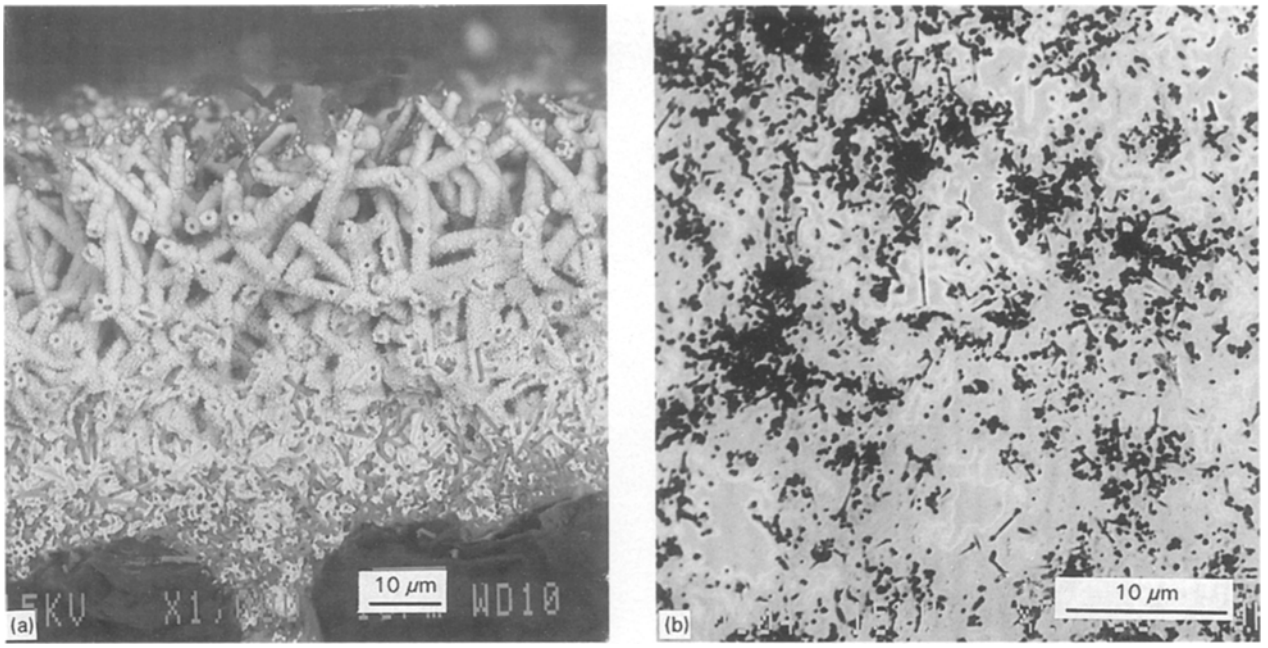

Figure 9 Specimen treated with Sn–Pd prior to infiltration by pulse plating (a) cross-section, (b) polished parallel to surface.

to adsorbed species on the growing nickel surface or gas bubbles trapped at the interface.

3.5. Hardness

Fig. 10 shows the hardness results as a function of whisker content for each of the electrodeposition conditions. Data for both d.c. and pulse plated nickel (with no whisker content) are also plotted. It is seen that there is no clear difference between the various plating conditions relative to the general scatter of the data. The presence of the whiskers increases the hardness to almost four times that of the plated nickel matrix material when a 50% whisker volume fraction is present. The results show an approximately linear relationship between hardness and whisker loading, although the slope is less than that expected from a true "rule of mixtures" as silicon carbide has a hardness of 2150–2950 KHN [28].

The whisker fraction varies with depth. Therefore, the penetration of the hardness indentor below the sample surface in principle will cause it to "see" a higher volume fraction of whiskers than that measured from the surface. However, the shallow indentation formed by the Knoop diamond minimizes this problem. Based on the measured indentation depths it has been calculated that the tip of the indentor experiences no more than approximately 1 vol % greater ceramic content. As the resistance to indentation will result from the entire indentation volume rather than just the tip, the systematic error due to this effect is small compared to the scatter of the hardness measurements.

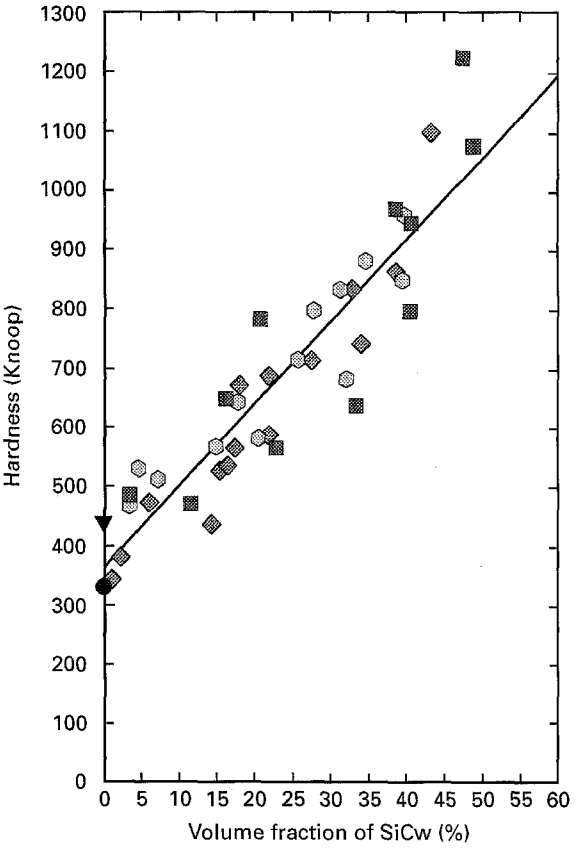

Figure 10 Knoop microhardness versus volume fraction of SiC whiskers for; (●) pure Ni, (▼) Pulse plated Ni, (◈) D.c. plated I = 5 mA per cm^2, (▩) Pulse plated 1 ms on 9 ms off I = 5 mA per cm^2 and (◎) SiC_w activated pulse plated 1 ms on 9 ms off, I = 5 mA per cm^2.

3.6. Sliding wear test

The results from the wear test are shown in Figs 11 and 12. The wear data is plotted as a ratio of the wear volume at a particular whisker volume fraction to that obtained with just the nickel matrix under the same test conditions. Fig. 11 shows the wear of the d.c. infiltrated samples. The data are widely scattered, especially at low whisker loadings. This can be attributed to the considerable porosity observed in these materials.

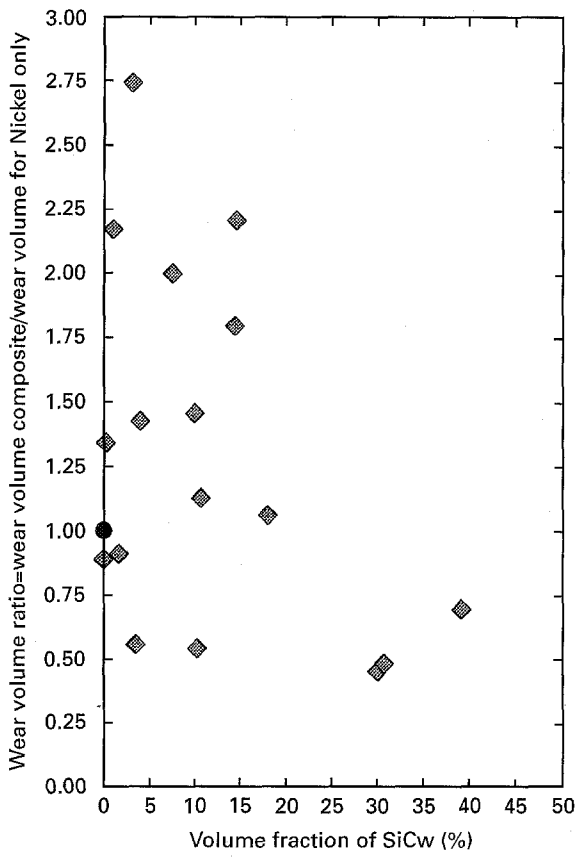

Figure 11 Relative wear volume versus whisker loading for d.c. infiltrated sample. The wear testing was performed on a pin-on-disk machine with a load of 500 g, a travel distance of 110 m at a speed of 1 cm per s. The samples investigated were; (●) pure Ni and (◈) D.c. plated at I = 5 mA per cm^2.

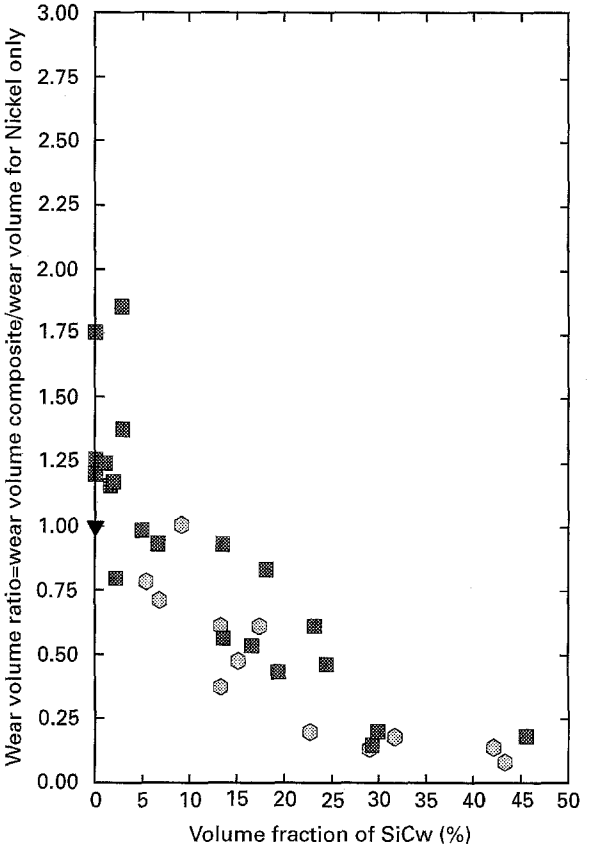

Figure 12 Relative wear volume versus whisker loading for composite made by pulsed-current infiltration. The wear testing was performed on a pin-on-disk machine with a load of 500 g a travel distance of 110 m at a speed of 1 cm per s. The samples studied were; (▼) pulse plated Ni, (▩) pulse plated at 1 ms on and 9 ms off I = 5 mA per cm^2 and (◍) SiC_w activated. Pulse plated 1 ms on and 9 ms off I = 5 mA per cm^2.

Fig. 12 gives the wear of pulse-plated samples, with results normalized to the wear of pulse-plated nickel. The general trend, as expected from the hardness data, is a significant reduction in wear with increased whisker content. Unlike the hardness data, the reduction in wear is not a linear function of whisker content. There is much less scatter in the results for whiskers infiltrated by pulse plating, however this did not hold true for non-activated (with Sn/Pd) samples at low whisker loadings. The activated samples had less scatter and had slightly lower wear. It is seen that the amount of wear levels off at approximately 30 vol %. At this loading the wear is approximately one sixth of that without whiskers present in the nickel. In comparison it has been reported [29] that wear of electroplated nickel was reduced to approximately one quarter by incorporation of 30 vol % SiC particles (22 μm average diameter).

As wear proceeds, the wear track will expose increasing whisker loading because of its variation with depth. Calculation has shown that the increased whisker fraction "seen" at the end of the wear test compared to that at the beginning varied from approximately 2.5 vol % larger for the 10 vol % loading (i.e. 25 % increase) to 1.5 vol % greater at 20 vol % to 0.6 vol % greater at 40 vol % (i.e. 1.5 % increase). Thus the error is significant for the lowest loadings but drops quickly to a relatively small value compared to the data scatter. This may explain the scatter at low loadings which may arise from the varying whisker content combined with non-uniformity of dispersion.

4. Summary

Nanophase SiC_w/Ni matrix composites have been synthesized by electrochemical infiltration of nickel into a CVD-grown SiC whisker mat. The latter was grown rapidly onto a graphite substrate by nickel catalysis via the vapour phase. Infiltration using direct current plating led to significant porosity and poor wear performance. Pulse plating significantly improved the infiltration process and resulted in reduced porosity and good wear results. The use of a tin–palladium surface treatment on the whiskers gave a further improvement.

Acknowledgements

The partial financial support of this work by the American Electroplaters and Surface Finishers Society through a summer grant (TJL) is acknowledged. Additional support was provided by the New Jersey Advanced Technology Centre for Surface Engineered Materials. We are grateful to Prof. T. Fischer for use of his tribology facility and to Dr. N. Wang for useful discussions.

References

1. T. VASILOS and E. G. WOLFF, *J. Metals* **18** (1986) 583.
2. P. K. ROHATGI, Y. LIU and S. RAY, "Friction, Lubrication and Wear Technology", ASM Handbook, Vol. 18, (American Society for Metals, 1990) p. 801.
3. "Fundamentals of Metal-Matrix Composites", Edited by S. Suresh, A. Mortensen and A. Needleman, (Butterworth-Heinemann, 1993).
4. A. MORTENSEN and M. J. KOCZAK, *J. Metals* **45** (1993) 10.
5. R. V. WILLIAMS and P. W. MARTIN, Proceedings of the 6th International Conference on Electrodeposition and Metal Finishing, p. 182, 1964.
6. A. A. BAKER, S. J. HARRIS and E. HOLMES, *Metals and Mat.* **1** (1967) 211.
7. W. A. WALLANCE and V. P. GRECO, *Plating* **57** (1970) 342.
8. J. C. WITHERS and E. F. ABRAMS, *ibid.* **55** (1968) 604.
9. I. AHMAD, V. P. GRECO and J. M. BARRANCO, *J. Composite Mat.* **1** (1967) 18.
10. V. P. GRECO, W. A. WALLACE and J. N. L. CESARO, *Plating* **56** (1969) 262.
11. R. N. HANSON, D. G. DUPREE and K. LUI, *ibid.* **55** (1968) 347.
12. V. P. GRECO, *Plating and Surface Finishing* **76** (1989) 62.
13. *Idem, ibid.* **76** (1989) 68.
14. P. SEARSON and T. P. MOFFAT, Critical Reviews in Surface Chemistry, 3(3/4) (1994), pp. 171–238.
15. J. LEE and I. B. CUTER, *Amer. Ceram. Soc. Bull.* **54** (1975) 195.
16. M. KAJIWARA, *J. Mater. Sci.* **21** (1986) 2254.
17. N. TAMARI, *J. Crystal Growth* **49** (1980) 199.
18. T. J. LEE, B. GALLOIS and K. SHEPPARD, to be published.
19. A. STORK, P. M. ROBERTSON and N. IBL, *Electrochimica Acta* **24** (1979) 373.
20. R. ALKIRE and P. K. NG, *J. Electrochem. Soc.* **124** (1977) 1220.
21. H. P. KIRCHNER and P. KNOLL, *J. Amer. Ceram. Soc.* **46** (1963) 299.
22. B. SUTTER in "Theory and Practice of Pulse Plating", Edited by J.-Cl. Puippe and F. Leaman (American Electroplaters and Surface Finishers Society, 1986) p. 101.
23. *Idem, ibid* p. 1 & p. 17.
24. D. L. REHRING, *Plating* **61** (1974) 43.
25. B. E. WARREN, *Progress in Metal Physics* **8** (1959) 147.
26. W. KLEINEKATHOFER and CH. J. RAUB, *Surface Technology* **7** (1978) 23.
27. C. de MINJER and P. F. J. van den BOOM, *J. Electrochem. Soc.* **120** (1973) 1644.
28. "ASM Engineered Materials Handbook", Vol. 4, "Ceramics and Glasses", 1991 (ASM International, 1991) p. 807.
29. M. GHOUSE, *Metal Finishing*, **82** (1984) 33.

Received 7 June 1995
and accepted 18 March 1996